Rapid Communication in Photoscience(2013), vol. 2, no. 3, pp.82-84
http://dx.doi.org/10.5857/RCP.2013.2.3.82
ISSN 2234-8182
eISSN 2288-4564

Communication

Preparation of TiO_2 Nanowires/Nanoparticles Composite Photoanodes for Dye-sensitized Solar Cells

Sung Yeon Heo, Won Seok Chi, Jin Kyu Kim, Chang Soo Lee, Jong Hak Kim*

Department of Chemical and Biomolecular Engineering, Yonsei University, 262 Seongsanno, Seodaemun-gu, Seoul 120-749, South Korea

ABSTRACT : We fabricated dye-sensitized solar cells (DSSCs) with TiO_2 nanowire (NW)/nanoparticle (NP) composite and solidified nanogel as the photoelectrode and electrolyte, respectively. TiO_2 NWs were generated via pore-infiltration of titanium (IV) isopropoxide (TTIP) into a track-etched polycarbonate membrane with a pore diameter of 100 nm, followed by calcination at 500℃. Energy conversion efficiency of TiO_2 NW/NP-based DSSCs was always higher than that of NP-based cells. We attributed this to improved light scattering and electron transport by TiO_2 NWs, as verified by intensity modulation photocurrent spectroscopy (IMPS) and intensity modulation photovoltage spectroscopy (IMVS) analyses. Quasi-solid-state DSSCs with NW/NP composites exhibited 5.0% efficiency at 100 mW/cm^2, which was much greater than that of NP-based cells (3.2%).

Dye-sensitized solar cells (DSSCs) have been researched intensively in the past two decades because of their low production cost, environmentally benign synthesis process, and high efficiency.[1] Basically, a DSSC consists of a TiO_2 photoanode, light absorbing dye, electrolyte containing a redox couple (I^-/I_3^-), and a Pt-coated counter electrode. Typically, photoanodes for DSSCs have been prepared using TiO_2 nanoparticles with a size range of 10-20 nm. However, slow electron transport through randomly-organized particulate TiO_2 film with a large grain boundary often leads to a tortuous electron path and increases the probability of recombination between injected electrons and electron acceptors in the redox species. Incorporation of one-dimensional nanostructures into nanoparticles has been proposed as a solution to solve the problems associated with randomly-organized nanoparticles.[2-5]

***To whom correspondence should be addressed.**
E-mail: jonghak@yonsei.ac.kr

In this study, we fabricated DSSCs by taking advantage of the synergistic effects of a solidified nanogel electrolyte and one-dimensional nanostructural photoanode to address the problems of electrolyte leakage and a tortuous electron path.[4] The photoanode was prepared by blending TiO_2 nanoparticles (NPs) and TiO_2 nanowires (NWs) generated using a track-etched polycarbonate membrane with a pore diameter of 100 nm as a template. We systematically examined the effect of the NW nanostructure and the nature of the electrolyte on the efficiency of DSSCs by analyzing current density-voltage (J-V) measurements and intensity modulation photocurrent spectroscopy/intensity modulation photovoltage spectroscopy (IMPS/IMVS) results.[6-9]

Polycarbonate membrane with a pore size of 100 nm was used as a template to generate TiO_2 NWs. Polycarbonate membranes are attractive to use because of simple removal by calcination, concomitant transformation from an amorphous precursor to crystalline phase, and lower cost than anodic aluminum oxide membranes, which require an additional step involving NaOH solution.[10,11] Immersion of polycarbonate membranes into a TTIP-based sol-gel solution results in infiltration of the TTIP precursor into the pores of the membranes due to capillary force. After calcination at 500℃, TiO_2 NWs with an outer diameter of 100 nm were generated **(Fig. 1a)**; this pore size is similar to the initial pore diameter of polycarbonate membrane, indicating that the polycarbonate acted as a structure-directing agent. The thickness of TiO_2 NP film was approximately 11 μm , which is slightly greater than the thickness (10 μm)

of TiO_2 NW/NP film. As shown in **Fig. 1c,** NWs were embedded in NPs with a less tightly packed structure, because the viscous paste containing the NPs was not able to penetrate deeply into the nanopores between the NWs. Furthermore, as shown in **Fig. 1d**, a large number of NWs were incorporated into the NPs in the form of bundles, likely due to strong van der Waals forces between NWs.

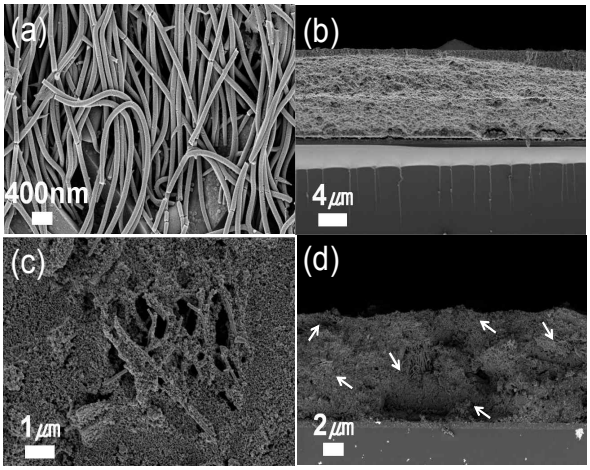

Figure 1. SEM images of (a) TiO_2 NWs templated by polycarbonate membranes, (b) TiO_2 NPs prepared from a paste, (c) TiO_2 NWs embedded in NPs, and (d) cross-sectional view of TiO_2 NWs/NPs.

Solar cell performances of DSSCs were measured at 100 mW/cm^2 using a solar simulator **(Fig. 2a)** and summarized in **Table 1.** Energy conversion efficiency of NW/NP-based cells with a I^-/I_3^- redox liquid electrolyte reached 5.5%, which is higher than that of NP-based cells (4.0%). Gel electrolyte DSSCs with NWs/NPs had efficiencies of 5.0% at 100 mW/cm^2, which is much greater than that of NP-based cells (3.2%). It should be noted that the efficiencies of NW/NP cells were always superior to those of NP cells. The J_{sc} values of TiO_2 NW/NP-based cells were always higher than those of bare TiO_2 NP cells. TiO_2 NWs were not closely packed with NPs, leading to a decrease in surface area, which is consistent with the dye adsorption measurements.[12] The amount of dye loaded on NW/NP films was 47.7 nmol/cm^2, which is slightly less than that loaded on NP films (51http://www.topten10.co.kr/magazine/showMailMagazine.lecs.5 nmol/cm^2). We assumed that the electron injection efficiencies of NP and NW/NP cells were very similar because we used the same electrolyte for both cell types.

Table 1. Photovoltaic parameters of DSSCs with N719 sensitizer under one sun condition of AM1.5 illumination.

Photoanode	Electrolyte	Dye loading (nmol/cm^2)	V_{oc} (V)	J_{sc} (mA/cm^2)	FF	η (%)
NPs	Liquid	51.5	0.83	7.7	0.62	4.0
NPs	Gel	51.5	0.89	5.9	0.60	3.1
NWs/NPs	Liquid	47.7	0.80	12.1	0.57	5.5
NWs/NPs	Gel	47.7	0.87	10.1	0.57	5.0

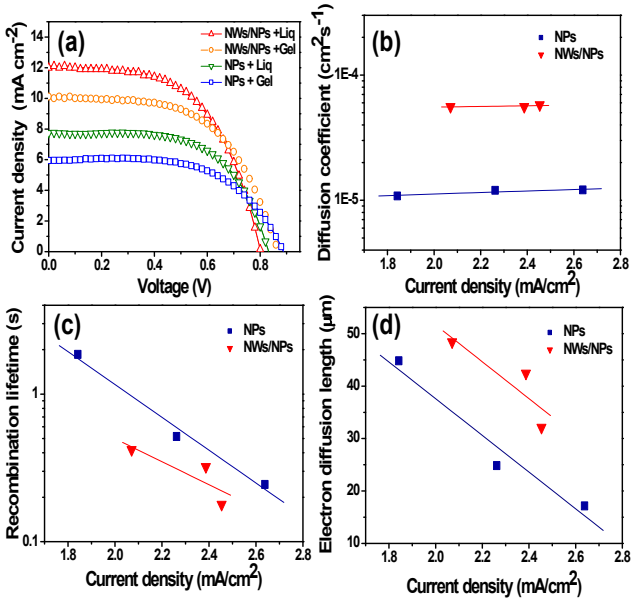

Figure 2. (a) J-V curves and IMPS/IMVS analysis of NP and NW/NP-based DSSCs: (b) diffusion coefficient, (c) recombination lifetime, and (e) electron diffusion length.

To investigate the electron collection efficiency of cells, IMPS/IMVS measurements were performed, as shown in **Fig. 2.** Electron diffusion coefficients of the NW/NP-based cells were much greater than those of the NP-based cells, as confirmed by IMPS/IMVS analysis. This demonstrates that electron transport is faster in one-dimensional NW/NP film than in film

containing randomly distributed NPs.[13] Recombination lifetime of NW/NP cells was lower than that of NPs cells, indicating that electrons in NW/NP composite films recombine more easily with I_3^- in the electrolyte and oxidized sensitizers.[14] This result is consistent with the lower FF and Voc values obtained for NW/NP cells than NP-based cells. Considering that the Voc value is mostly determined by the difference in Fermi level of the TiO_2 photoanode and the redox potential of the electrolyte, the increased recombination in NW/NP-based cells might decrease the electron density in TiO_2 films, resulting in a decreased $V_{oc.}$ Electron diffusion length was calculated using the electron diffusion coefficient and recombination lifetime. At the same current density, the electron diffusion length of NW/NP cells was much larger than that of NP cells, indicating better electron collection efficiency in the former. Thus, we concluded that the high J_{sc} value of NW/NP cells could be explained by enhanced light scattering by NWs and faster electron transport through the NWs.

KEYWORDS: dye-sensitized solar cells; nanowires; nanogel electrolyte;TiO_2.

Received October 29, 2013; Accepted 17, December 2013

ACKNOWLEDGEMENT

We acknowledge the financial support of the Pioneer Research Center Program (2008-05103), the Core Research Program (NRF-2012R1A2A2A02011268), and the Korea Center for Artificial Photosynthesis (KCAP) (NRF-2011-C1AAA001-2011-0030278).

REFERENCES AND NOTES

1. Oregan, B.; Gratzel, M. *Nature*, **1991,** 353, 737-740.
2. Tan, B.; Wu, Y. Y. *J. Phys. Chem. B,* **2006,** 110, 15932-15938.
3. Bai, Y.; Yu, H.; Li, Z.; Amal, R.; Lu, G. Q.; Wang, L. Z. *Adv. Mater.* **2012,** 24, 5850-5856.
4. Park, J. T.; Koh, J. H.; Seo, J. A.; Kim, J. H. *J. Mater. Chem.* **2011,** 21, 17872-17880.
5. Tian, G. H.; Pan, K.; Chem, Y. J.; Zhou, J.; Miao, X. H.; Zhou, W.; Wang, R. H.; Fu, H. G. *J. Power Sources,* **2013,** 238, 350-355.
6. Ahn, S. H.; Chi, W. S.; Park, J. T.; Koh, J. K.; Roh, D. K.; Kim, J. H. *Adv. Mater.* **2012,** 24, 519-522.
7. Ahn, S. H.; Koh, J. H.; Seo, J. A.; Kim, J. H. *Chem. Commun,* **2010,** 46, 1935-1937;
8. Chi, W. S.; Koh, J. K.; Ahn, S. H.; Shin, J. S.; Ahn, H.; Ryu, D. Y.; Kim, J. H. *Electrochem. Commun,* **2011,** 13, 1349-1352.
9. Koh, J. K.; Koh, J. H.; Ahn, S. H.; Kim, J. H.; Kang, Y. S. *Electrochim. Acta,* **2010,** 55, 2567-2574.
10. Roh, D. K.; Patel, R.; Ahn, S. H.; Kim, D. J.; Kim, J. H. *Nanoscale,* **2011,** 3, 4162-4169.
11. Bae, C. D.; Kim, S. Y.; Ahn, B. Y.; Kim, J. Y.; Sung, M. M.; Shin, H. J. *J. Mater. Chem.* **2008,** 18, 1362-1367.
12. Park, J. T.; Prosser, J. H.; Kim, D. J.; Kim, J. H.; Lee, D. *Chemsuschem,* **2013,** 6, 856-864.
13. Zhu, K.; Neale, N. R.; Miedaner, A.; Frank, A. J. *Nano. Lett.* **2007,** 7, 69-74.
14. Ohsaki, Y.; Masaki, N.; Kitamura, T.; Wada, Y.; Okamoto, T.; Sekino, T.; Niihara, K.; Yanagida, S. *Phys. Chem. Chem. Phys.* **2005,** 7, 4157-4163.